Am J Cancer Res 2021;11(4):1540-1556
www.ajcr.us /ISSN:2156-6976/ajcr0129288

Original Article

Low miR-16 expression induces regulatory CD4$^+$NKG2D$^+$ T cells involved in colorectal cancer progression

Tao Zhu[1,2*], Zhijie Lin[1,2*], Sen Han[1,2], Yingying Wei[2,4], Guotao Lu[3], Yu Zhang[2,4], Weiming Xiao[2,3,4], Zhengbing Wang[2,3,4], Xiaoqin Jia[2,5], Weijuan Gong[1,2,3,4,5]

[1]Department of Immunology, School of Medicine, Yangzhou University, Yangzhou 225001, Jiangsu Province, P. R. China; [2]Jiangsu Key Laboratory of Integrated Traditional Chinese and Western Medicine for Prevention and Treatment of Senile Diseases, Yangzhou 225001, Jiangsu Province, P. R. China; [3]Department of Gastroenterology, Affiliated Hospital, Yangzhou University, Yangzhou 225001, Jiangsu Province, P. R. China; [4]Jiangsu Key Laboratory of Zoonosis, Yangzhou 225001, Jiangsu Province, P. R. China; [5]Jiangsu Co-innovation Center for Prevention and Control of Important Animal Infectious Diseases and Zoonoses, Yangzhou 225001, Jiangsu Province, P. R. China. [*]Equal contributors.

Received December 30, 2020; Accepted February 1, 2021; Epub April 15, 2021; Published April 30, 2021

Abstract: MiR-15a/16 is a member of the miRNA cluster that exhibits tumor suppression and immune modulation via targeting multiple genes. Decreased miR-15a/16 expression is involved in many cancer cells. Here, miR-16 had decreased expression in NK1.1$^-$CD4$^+$NKG2D$^+$ T cells and bound with the 3'-UTR of *NKG2D* gene. MiR-15a/16-deficient mice had many CD4$^+$NKG2D$^+$ T cells, which produced TGF-β1 and IL-10 and inhibited the IFN-γ production of CD8$^+$ T cells. Adoptive transfer of NK1.1$^-$CD4$^+$NKG2D$^+$ T cells from miR-15a/16-deficient mice promoted tumor growth *in vivo*. However, no changes for NK1.1$^-$CD4$^+$NKG2D$^+$ T cells were found in the miR-15a/16-transgenic mice. Although the miR-15a/16 transgenic mice transplanted with B16BL6 or MC38 cells exhibited rapid growth, these tumor-bearing mice did not show changes in NK1.1$^-$CD4$^+$NKG2D$^+$ T cell distributions in either spleens or tumors. When NK1.1$^-$CD4$^+$ T cells were stimulated by α-CD3/sRAE-1 *ex vivo*, the NKG2D expression was difficult to induce in the T cells of miR-15a/16-transgenic mice. Finally, increased frequencies of regulatory CD4$^+$NKG2D$^+$ T cells with low miR-16 levels were observed in patients with late-stage colorectal cancer (Duke's C, D). Thus, miR-16 modulates NK1.1$^-$CD4$^+$NKG2D$^+$ T cell functions via targeting NKG2D. Low miR-16 expression in CD4$^+$ T cells induces the regulatory CD4$^+$NKG2D$^+$ T subpopulation, which promotes tumor evasion via the secretion of immune-suppressive molecules.

Keywords: miR-15a/16, CD4$^+$ T cell, NKG2D, colorectal cancer, regulation

Introduction

Since the discovery of the correlation between miR-15a/16 cluster and poor prognosis in chronic lymphocytic leukemia in 2002, the biologic features of miR-15a/16 have been widely investigated [1]. MiR-15a/16 is mostly regarded as a tumor suppressor by targeting oncogenic genes that regulate the cell cycle, survival, epithelial-mesenchymal transition, and angiogenesis [2, 3]. Decreased miR-15a/16 levels are observed in colorectal cancer [4], hepatoma [5], bladder cancer [6], prostate cancer [7], and different kinds of lymphoma [8] or leukemia [9]. Bioinformatics analysis revealed more than 1,000 target genes of miR-15a/16. Its expression is promoted by p53 [10] and all-trans retinoic acid (ATRA) [11] but repressed by c-Myc [12], hypoxia-induced factor (HIF)-1 and anaplastic lymphoma kinase [13], activating protein 4 (AP4) [10], protein arginine deiminase [14], human epidermal growth factor receptor-2 (HER2) [15], and histone deacetylase (HDAC) 3 [16, 17].

Owing to their shared identical seed sequences, miR-15a and miR-16 are assigned to the same miRNA family. The anti-inflammatory activity of miR-15a/16 inhibits macrophage activation via targeting programmed cell death 4 (PDCD4) [18] and mitogen-activated protein kinase (MAPK) [19] and NF-κB pathways [20]. MiR-16 also transforms macrophages from M2 to M1 [21]. MiR-15a/16 deficiency promotes B

cell proliferation by accelerating the G0/G1-S phase transition [22] and induces IL-10 production by regulatory B cell due to STAT3 activation [23]. miR-15a/16 also modulates T cell function via targeting mTOR/Rictor [24] or IKKα [25] or regulates memory T cell generation by targeting IL-7 receptor (CD127) and CD28 [26].

NK1.1-CD4+NKG2D+ T cells promote tumor growth [27] and ameliorate DSS-induced colitis [28] by downregulating effector T cells, NK cells [29], and macrophages that are dependent on TGF-β1, IL-10, and Fas ligand. The coligation of CD3 and NKG2D stimulates NK1.1-CD4+NKG2D+ T cells to secret TGF-β1 via the activation of PI3K-p85α/Jnk, NF-κB, STAT3, and Egr2/3 pathways [30, 31]. Bioinformatics analysis indicated that miR-16 binds to the 3'-untranslated regions (3'-UTR) of the NKG2D gene. Whether miR-16 could directly target NKG2D and thus modulate the activities of NK1.1-CD4+NKG2D+ cells was investigated in this study. The relevance of regulatory CD4+NKG2D+ T cells modulated by miR-16 in patients with colorectal cancer (CRC) was also discussed.

Materials and methods

Mice and reagents

MiR-15a/16-/- mice (KO) were purchased from the Jackson Laboratory (Bar Harbor, Maine, USA). MiR-15a/16-transgenic mice (TG) were provided by the Gem Pharmatech Company (Nanjing, China). All mice were reared in the Comparative Medical Center of Yangzhou University. All animal experimental protocols were approved by the Institutional Animal Care and Ethics Committee of Yangzhou University, Yangzhou, China (Approval ID: SYXK [Su] 2017-0044). MC38, 293T, and B16BL6 cell lines were obtained from the ATCC (Manassas, VA, USA). Cells were cultured in DMEM or RPMI 1640 medium (supplemented with 10% fetal bovine serum, streptomycin-penicillin).

The following reagents were used: soluble RAE-1 (R&D, Minneapolis, MN, USA) and recombinant IL-2, IL-21, IL-15, IL-4, IL-6, and TGF-β1 (Biolegend, San Diego, CA, USA). The following antibodies against mouse antigens were purchased from Biolegend or eBioscience (San Diego, CA, USA): CD3 (145-2C11), CD28 (37.51), CD4 (GK1.5), NKG2D (CX5), CD8 (53-6.7), NK1.1 (PK136), IL-10 (JES5-16E3), TGF-β1 (TW7-16B4), IFN-γ (XMG1.2), CD107a (ID4B), CD69 (H1.2F3), CD44 (IM7), CD25 (3C7), and CD28 (E18). Antibodies against human CD3 (OKT3), CD4 (OKT4), NKG2D (1D11), IL-10 (JES3-19F1), and TGF-β1 (TW4-6H10) were also employed.

Flow cytometry

For the detection of surface markers, the cells were incubated with indicated antibodies and analyzed by flow cytometry. For the measurement of intracellular cytokines, the cells were harvested, fixed, permeabilized with intracellular fixation buffer and permeabilization buffer, stained with the appropriate antibodies, and analyzed by flow cytometry. For the measurement of lymphocyte degranulation, anti-CD107a mAb was added to mixed culture systems for 2 hours, and monensin (GolgiStop; BD Biosciences) was then added for another 2 hours. The cells were collected and stained by surface markers for flow cytometry.

Real-time PCR

TRIzol reagent (Invitrogen) was utilized to extract the total RNA of mouse NK1.1-CD4+NKG2D+ or human CD3+CD4+NKG2D+ cells. Reverse transcription was completed using a PrimeScript RT reagent kit (TaKaRa, Japan). Real-time polymerase chain reaction (PCR) was performed routinely. U6 was used as an internal reference for miR16, and 2-ΔΔCt method was utilized to calculate the expression values of miR-16 and NKG2D. The primer sequences were as follows: NKG2D forward (5'-CCACTGCCAGGAGCCATTT-3') and NKG2D reverse (5'-ACTGTGGCCCATGCCCTAA-3'); GAPDH forward (5'-CAAAATGGTGAAGGTCGGTGTG-3') and GAPDH reverse (5'-TGATGTTAGTGGGGTCTCGCTC-3'); miR-16 (mouse) sense (5'-TAGCAGCACGTAAATATTGGCG-3') and miR-16 (human) sense (5'-GTCAGCAGTGCCTTAGCAG-3'); and U6 forward (5'-TGGAACGCTTCACGAATTTGC-3') and reverse (5'-GGAACGATACAGAGAAGATTAGC-3').

Dual-luciferase assays

Gene sequences (wild type or mutated, Figure S1) of NKG2D 3'-UTR were cloned into the pGL3-basic vector with dual fluorescein reporter. Sequences of miR-16 mimics (20 pmol)

were synthesized by Sangon Biotech (Shanghai, China). The cells were cotransfected with the cloned pGL3 vector and miR-16 mimics. Transfection was performed using Lipofectamine 3000 (Invitrogen) following the manufacturers' instructions. After 48 hours, the cells were collected and analyzed using the Dual-luciferase Reporter Assay System (Promega). The cloning sequences of NKG2D-3'-UTR were as follows: forward (5'-ACACGAATTCTGGTGCTGGAAGGAGTTGT-3') and reverse (5'-ACACTCTAGAAGGTCATTGTGCAGGTTGTA-3').

Tumor growth in mice

B16BL6 or MC38 (2×10^6) cells were implanted subcutaneously into the back of wild-type mice and miR-15a/16-transgenic mice. Tumor volume was determined by its dimensions and width using the following formula: $V = 1/2$ length × width^2. In the adoptive transfer experiments, NK1.1$^-$CD4$^+$NKG2D$^+$ cells (1×10^6) were sorted out and then injected into tail veins twice per week [27].

Patients and biopsies

Fifty-two patients with CRC (35 males and 17 females) with age ranging from 27 years to 82 years (mean, 65.6±10.2) and twenty-one healthy controls (14 males and 7 females, mean age 42.4±9.8 years) were recruited. Before peripheral blood mononuclear cells were collected, the patients did not get any surgery, chemotherapy, or radiotherapy. Biopsy collection was approved by the Institutional Review Board of Yangzhou University. All patients signed informed consents. The clinical characteristics of patients with CRC are shown in Table S1.

Statistical analysis

Continuous variables were presented as means ± SD. Differences between the two groups were analyzed in unpaired, two-tailed Student's *t*-tests. MiR-16 expression levels were compared between CD4$^+$NKG2D$^-$ and CD4$^+$NKG2D$^+$ cells of the same individual by using paired Student's *t*-tests. Data from more than two groups were analyzed by one-way ANOVA, followed by Dunnett's test to compare the control and multiple treatment groups. Linear regression was used to analyze the correlation of two variables. Statistical significance was indicated as *, $P < 0.05$; **, $P < 0.01$; and ***, $P < 0.001$.

Results

MiR-16 downregulation in NK1.1$^-$CD4$^+$NKG2D$^+$ T cells

NKG2D expression was normally induced when mouse NK1.1$^-$CD3$^+$CD4$^+$ cells were stimulated with α-CD3, or sRAE-1, or α-CD3/sRAE-1, or α-CD3/α-CD28 *ex vivo* [30, 31]. Stimulation with α-CD3/sRAE-1 could most efficiently induce CD4$^+$NKG2D$^+$ cells (**Figure 1A** and **1B**). The highest reduction in miR-16 transcription in CD4$^+$NKG2D$^+$ cells was induced by the treatment of α-CD3/sRAE-1 (**Figure 1C**). The ability of IL-2, IL-21, or IL-15 to induce the NKG2D expression of CD4$^+$ cells was lower than that of α-CD3. IL-4 or IL-6/TGF-β1 could not increase the NKG2D expression of CD4$^+$ cells (**Figure 1C**). However, the NKG2D transcriptional level was enhanced by all the treatments of α-CD3, IL-2, IL-21, IL-15, IL-4, or IL-6/TGF-β1 (**Figure 1D**). Meanwhile, the miR-16 levels were decreased after the CD4$^+$ cells were activated by the above cytokines (**Figure 1E**). In summary, miR-16 was negatively associated with the NKG2D expression of CD4$^+$ cells. Differences of NKG2D mRNA and protein levels in CD4$^+$ cells induced by the treatment of IL-4 or IL-6/TGF-β1 indicated that NKG2D expression was regulated at the post-transcriptional level.

MiR-16 targets the 3'-UTR of NKG2D

Given the miR16-complementary sequences in the 3'-UTR of *NKG2D* (**Figure 2A**), whether miR-16 could directly bind with target sequences was determined by dual-luciferase reporter assay. Native or mutated sequences of NKG2D 3'-UTR were cloned into pGL3 vectors (**Figure 2B**). As shown in **Figure 3C** and **3D**, the luciferase activity was substantially decreased when miR-16 and pGL3-NKG2D-3'-UTR native were co-transfected into 293 T cells but was restored when miR-16 and pGL3-NKG2D-3'-UTR mutated were co-transfected into 293 T cells. These results revealed that miR-16 binds with the 3'-UTR of NKG2D.

Increased regulatory CD4$^+$NKG2D$^+$ T cells in miR-15a/16$^{-/-}$ mice

Variations of NK1.1$^-$CD3$^+$CD4$^+$NKG2D$^+$ cells in the miR-15a/16$^{-/-}$ mice were also examined. The frequencies of CD4$^+$NKG2D$^+$ T subsets were increased in miR-15a/16$^{-/-}$ mice at the

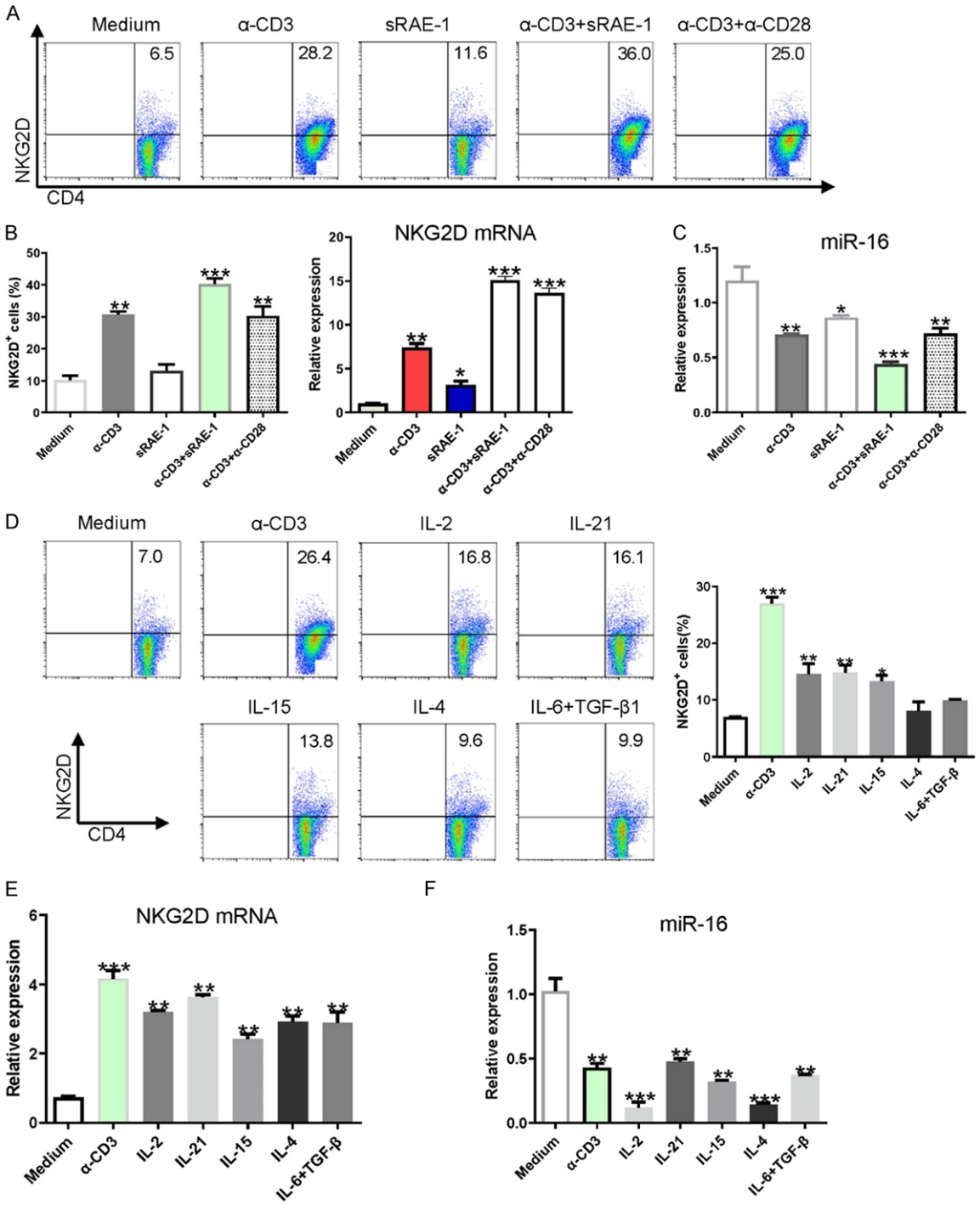

Figure 1. Decreased miR-16 expression in CD4+NKG2D+ T cells induced by α-CD3/sRAE-1. A, B. NKG2D expression of NK1.1-CD3+CD4+ cells induced by different treatments. C. MiR-16 levels in CD4+NKG2D+ T cells induced by various stimulations as detected by real-time PCR. D. NKG2D expression on NK1.1-CD3+CD4+ cells induced by various cytokines. E. NKG2D transcriptions on NK1.1-CD3+CD4+ cells treated by cytokines. F. Variations of miR-16 levels in CD4+NKG2D+ T cells. All experiments were repeated twice. *, $P < 0.05$; **, $P < 0.01$; *ns*, no significance.

age of 8-12 weeks or 12-15 months (**Figure 3A**). Considering that the aged miR-15a/16$^{-/-}$ mice could develop chronic lymphocyte leukemia [9], whether the tumor microenvironment induces CD4+NKG2D+ T cells was analyzed. MC38 cells (colon cancer) were transplanted

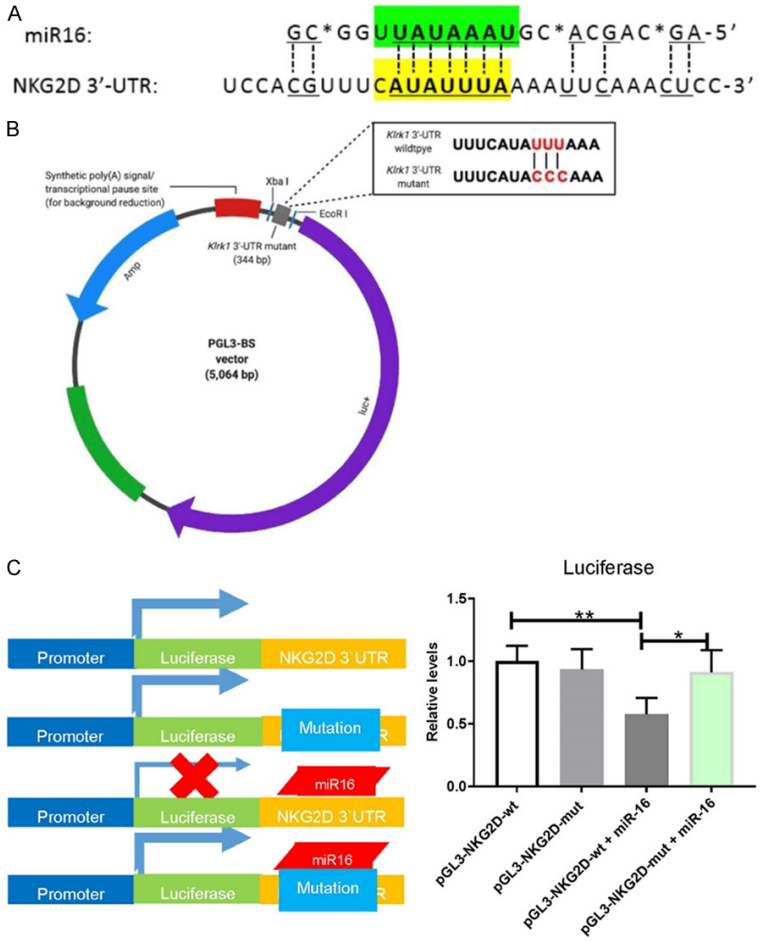

Figure 2. MiR-16 binding with NKG2D 3'-UTR. A. Nucleotide pairs of miR-16 and NKG2D 3'-UTR. B. Cloning of native and mutated 3'-UTR into the pGL3 vector. C. Luciferase reporter assay with miR-16 mimics and recombinant pGL3 plasmids co-transfection. Transfection experiments were conducted three times. *, $P < 0.05$; **, $P < 0.01$.

into the young miR-15a/16$^{-/-}$ mice and wild-type mice. Compared with those in wild-type mice, the CD4$^+$NKG2D$^+$ T cell frequencies were more remarkably enhanced in the tumor-bearing miR-15a/16$^{-/-}$ mice (**Figure 3B**), thus confirming that the miR-15a/16 deletion induces CD4$^+$NKG2D$^+$ T cells.

The CD4$^+$NKG2D$^+$ T cells of miR-15a/16$^{-/-}$ mice produce TGF-β1 and IL-10. Differences in TGF-β1 production were exhibited by CD4$^+$NKG2D$^+$ T cells (**Figure 3C**). When CD8$^+$ T cells were incubated with the CD4$^+$NKG2D$^+$ T cells of KO mice, the IFN-γ production of CD8$^+$ T cells was decreased. However, when TGF-β1 antibody was added into the co-culture system, the ability of CD8$^+$ T cells to secret IFN-γ was almost recovered (**Figure 3D**). Fast tumor growth was observed when the CD4$^+$NKG2D$^+$ T cells of miR-15a/16$^{-/-}$ mice were adoptively transfused into wild-type mice transplanted with MC38 cells (**Figure 3E**). These results indicated the immune-regulatory function of CD4$^+$ NKG2D$^+$ T cells induced by miR-15a/16 deficiency.

NKG2D expression on NK1.1$^-$ CD4$^+$ cells in miR-15a/16-TG mice

The effect of miR-16 overexpression on the activities of regulatory CD4$^+$NKG2D$^+$ T cells was investigated. In consideration of the low efficiency of transfection into CD4$^+$ T cells using lentivirus, miR-15a/16-transgenic mice were established. The open reading frame of miR-15a/16 linked with green fluorescent protein (GFP) was introduced into the germline of C57BL/6 mice (**Figure 4A**). Offspring with high expressions of GFP in tail vein cells were selected and backcrossed. Two transgenic lines (Lines 3 and 11) were established for further study. Increased miR-16 levels were confirmed in the tissues of gut, lung, liver, and stomach (**Figure 4B**). The GFP$^+$ cells of tail veins were detected and are shown in **Figure 4C**.

The elevated miR-16 level in CD4$^+$ T cells of TG mice and the low miR-16 expression in CD4$^+$ T cells of KO mice were verified (**Figure 4D**). The NKG2D mRNA level of CD4$^+$ T cells was increased in KO mice but decreased in TG mice (**Figure 4E**). Although CD4$^+$NKG2D$^+$ T cell frequencies were increased in KO mice, no differences in CD4$^+$NKG2D$^+$ T cell frequencies were observed between TG and WT mice (**Figure 4F**). CD69, CD44, CD25, and CD28 were also checked to determine other genes in CD4$^+$ T cells being targeted by miR-16. The expression levels CD69, CD44, and CD25 were upregulated in miR-15a/16-deficient CD4$^+$ T cells but were not changed in CD4$^+$ T cells with overexpressed miR-15a/16. No ch-

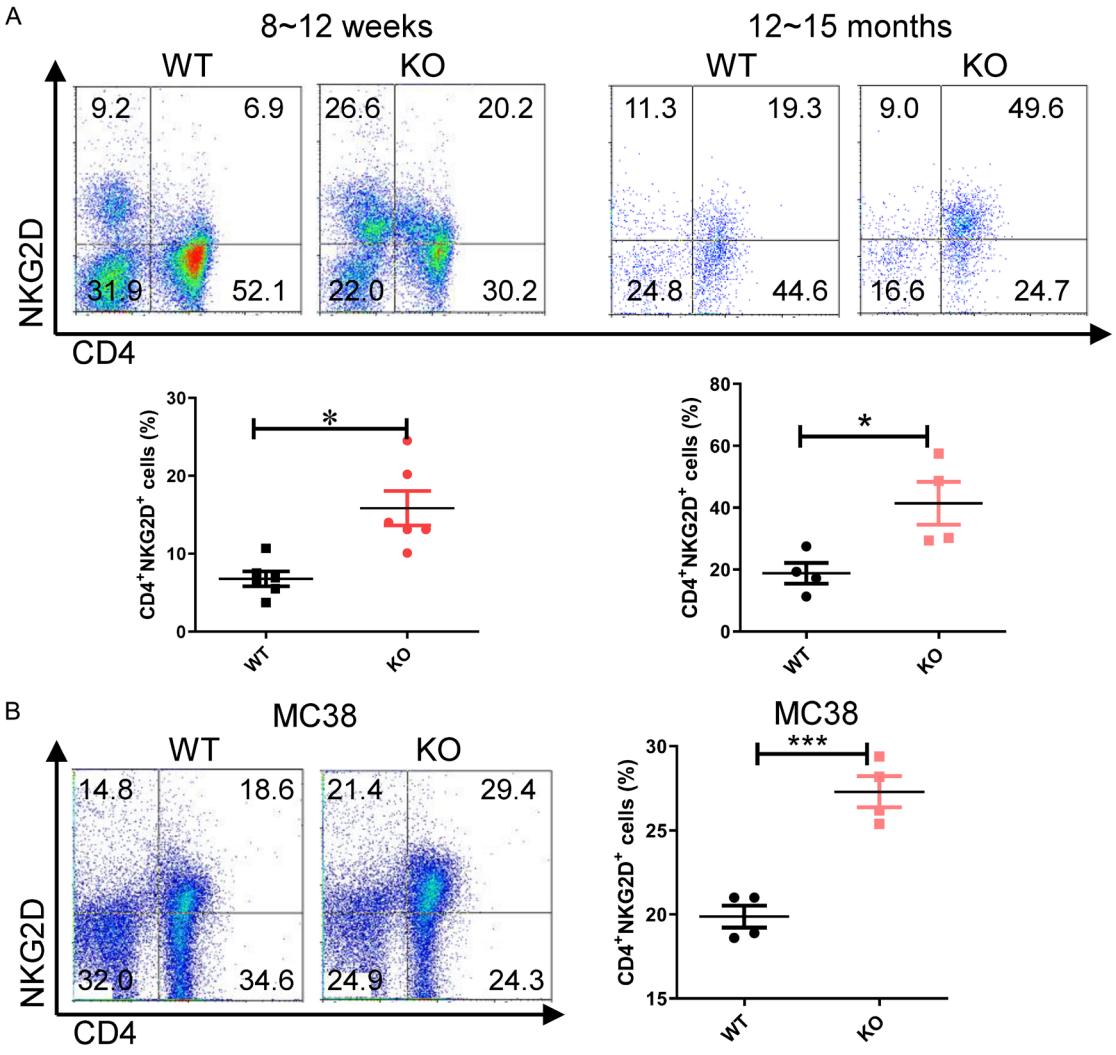
A
8~12 weeks
12~15 months
WT
KO
WT
KO
9.2
6.9
31.9
52.1
26.6
20.2
22.0
30.2
11.3
19.3
24.8
44.6
9.0
49.6
16.6
24.7
NKG2D
CD4
CD4⁺NKG2D⁺ cells (%)
*
*
B
MC38
MC38
WT
KO
14.8
18.6
32.0
34.6
21.4
29.4
24.9
24.3
***
NKG2D
CD4

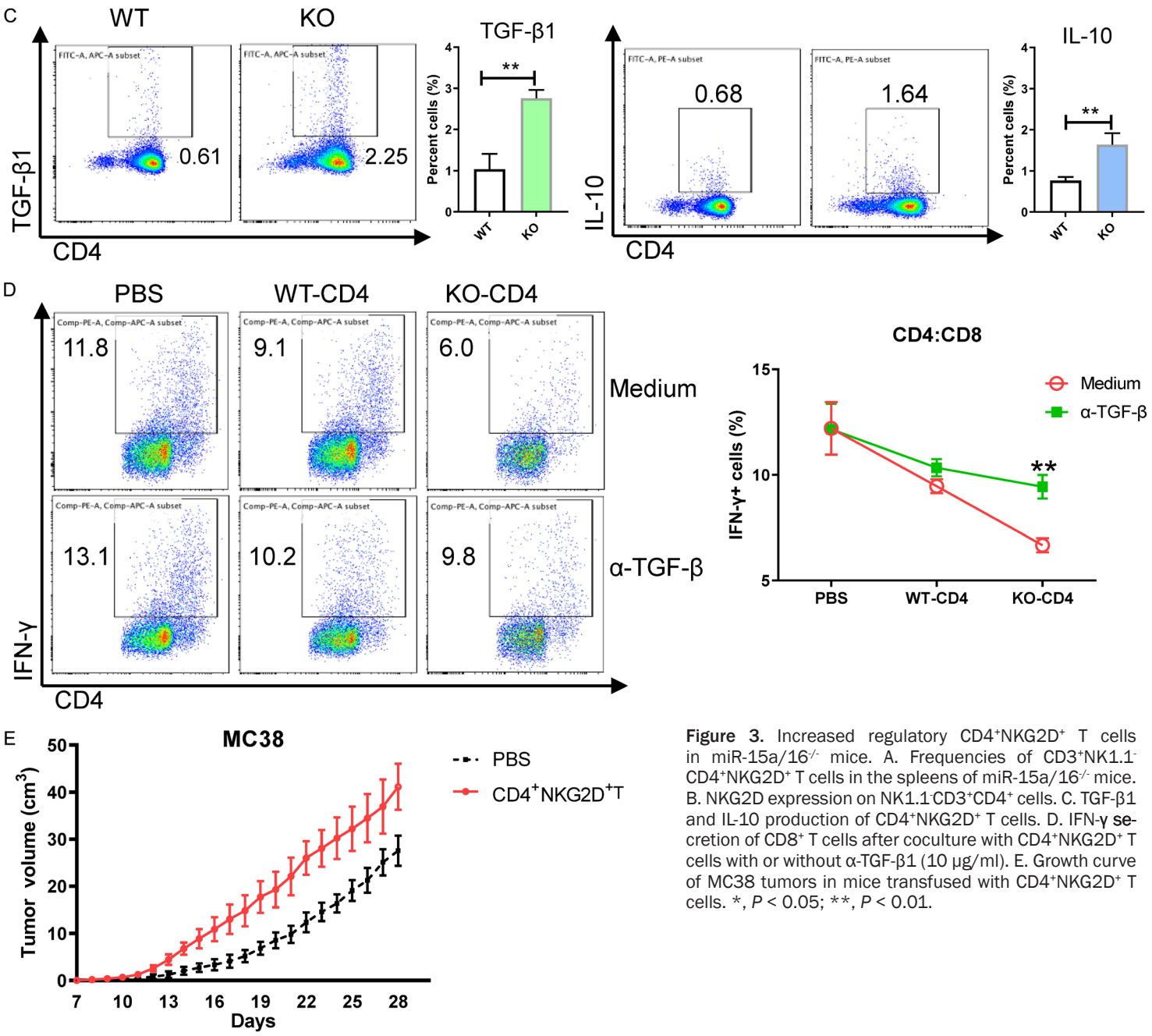

Figure 3. Increased regulatory CD4⁺NKG2D⁺ T cells in miR-15a/16$^{-/-}$ mice. A. Frequencies of CD3⁺NK1.1⁻CD4⁺NKG2D⁺ T cells in the spleens of miR-15a/16$^{-/-}$ mice. B. NKG2D expression on NK1.1⁻CD3⁺CD4⁺ cells. C. TGF-β1 and IL-10 production of CD4⁺NKG2D⁺ T cells. D. IFN-γ secretion of CD8⁺ T cells after coculture with CD4⁺NKG2D⁺ T cells with or without α-TGF-β1 (10 μg/ml). E. Growth curve of MC38 tumors in mice transfused with CD4⁺NKG2D⁺ T cells. *, $P < 0.05$; **, $P < 0.01$.

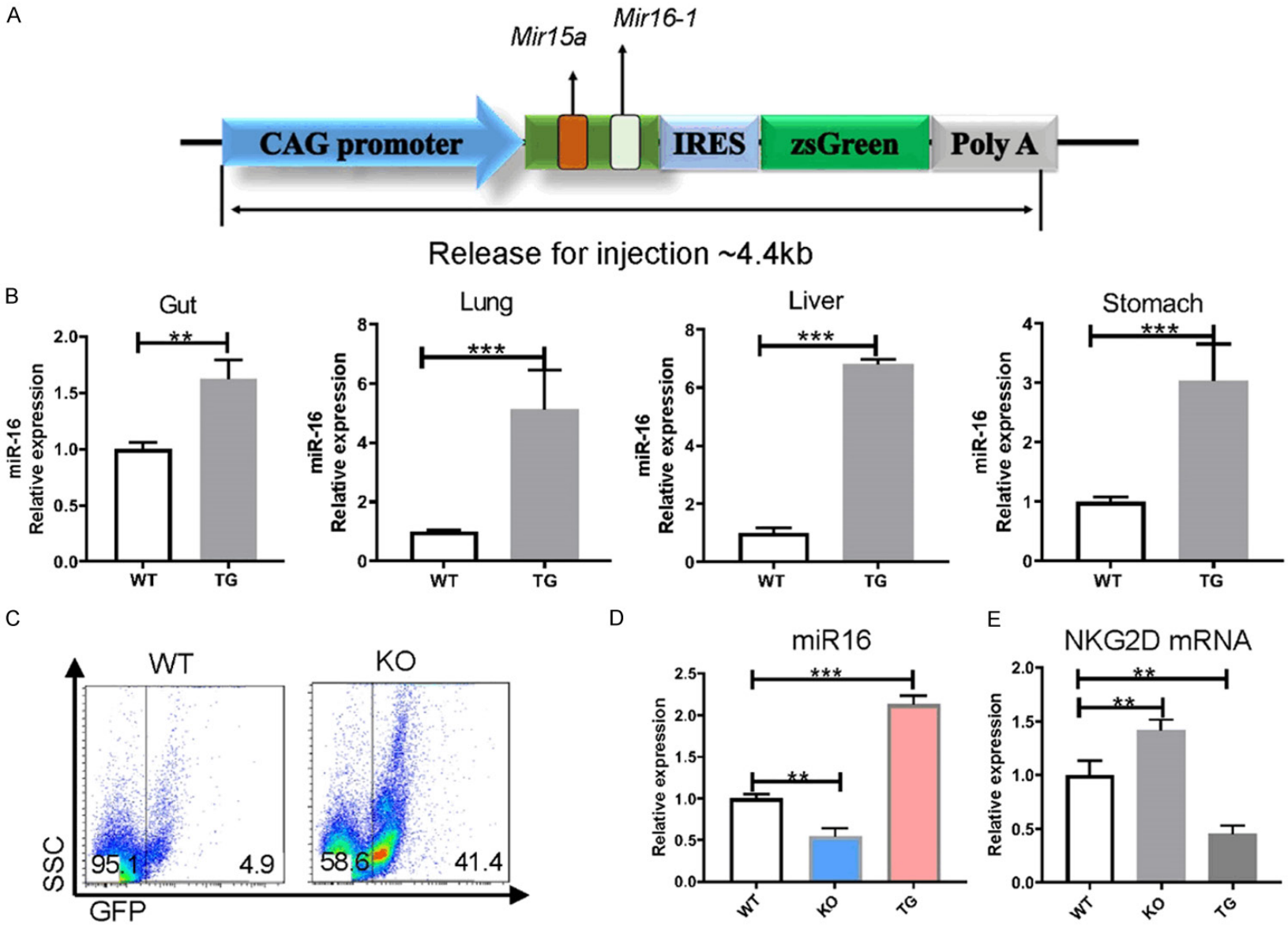
A
Mir15a
Mir16-1
CAG promoter
IRES
zsGreen
Poly A
Release for injection ~4.4kb
B
Gut
Lung
Liver
Stomach
miR-16 Relative expression
WT
TG
C
WT
KO
SSC
GFP
95.1
4.9
58.6
41.4
D
miR16
Relative expression
WT
KO
TG
E
NKG2D mRNA
Relative expression
WT
KO
TG

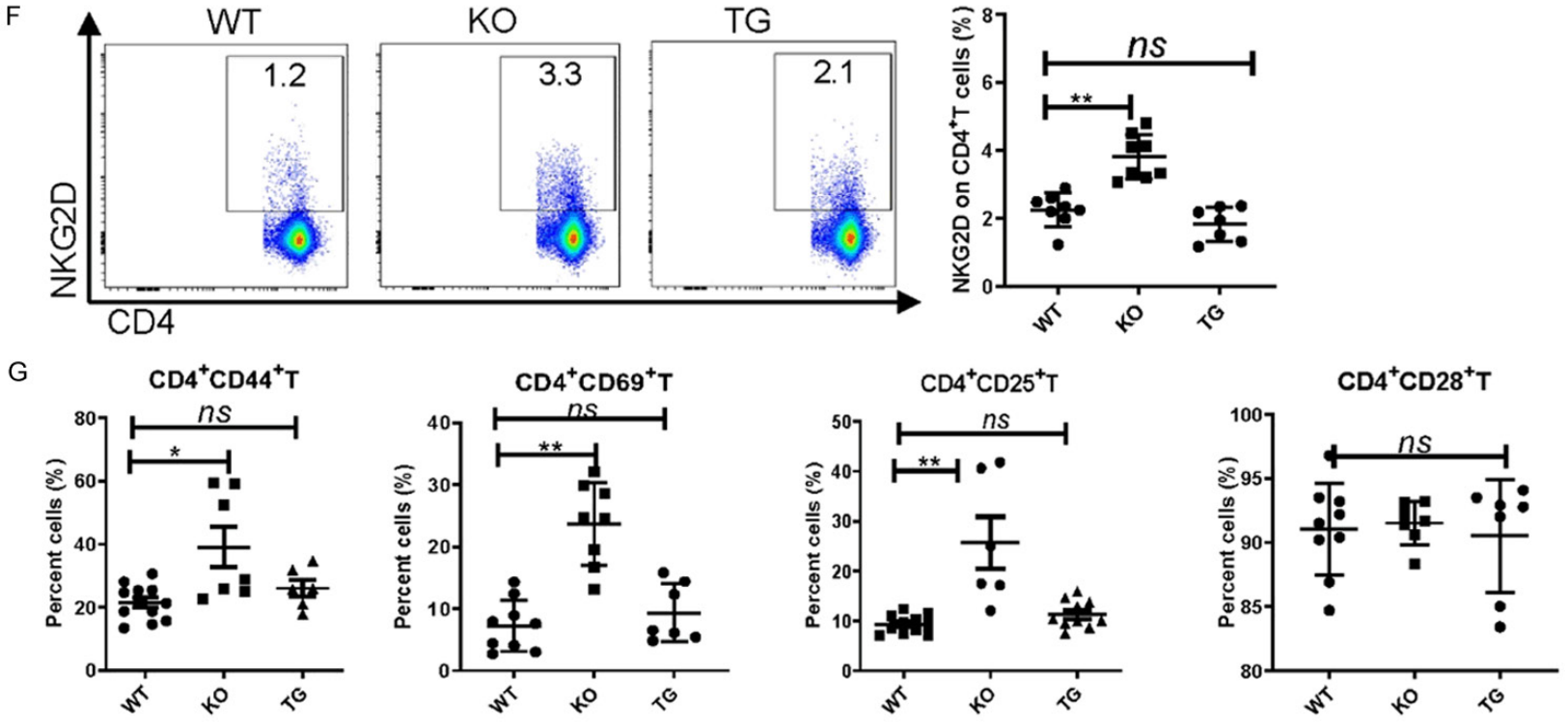
F
WT
KO
TG
1.2
3.3
2.1
NKG2D
CD4
NKG2D on CD4⁺T cells (%)
ns
**
G
CD4⁺CD44⁺T
CD4⁺CD69⁺T
CD4⁺CD25⁺T
CD4⁺CD28⁺T
Percent cells (%)
*

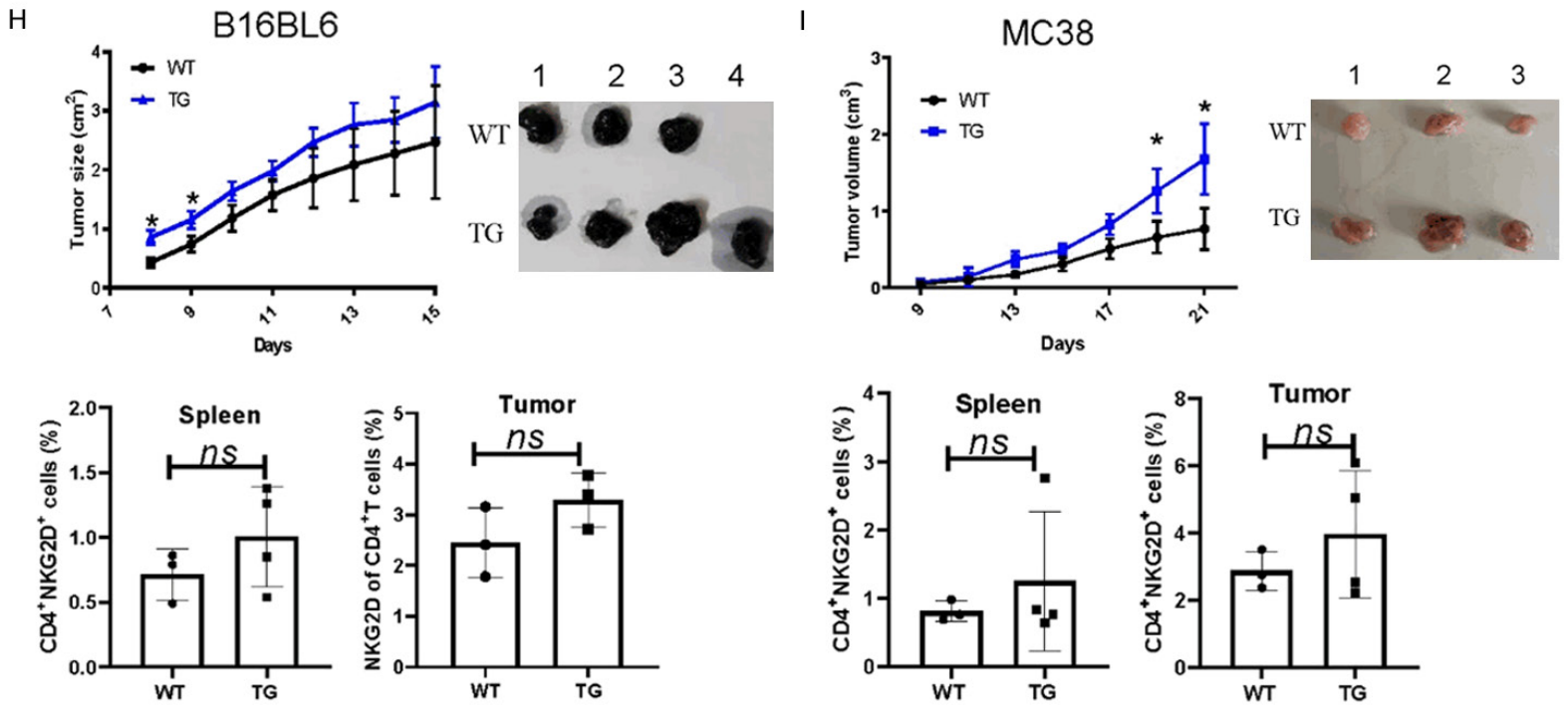

Figure 4. Variations of CD4⁺NKG2D⁺ T cells in miR-15a/16-transgenic mice. (A) Diagram of the gene element for microinjection. (B) MiR-16 levels in the tissues of gut, lung, liver, and stomach. (C) GFP⁺ cells in tail veins of transgenic mice. (D) MiR-16 levels of CD4⁺NKG2D⁺ T cells in WT, KO, and TG mice. (E) Transcriptional levels of NKG2D in CD4⁺ T cells of three mouse groups. (F) NKG2D protein levels on CD4⁺ T cells of three groups of mice. (G) Frequencies of CD4⁺CD69⁺, CD4⁺CD44⁺, CD4⁺CD25⁺, and CD4⁺CD28⁺ T cells in three mouse groups. Growth of transplanted B16BL6 (H) and MC38 (I) cells in the transgenic mice and distributions of CD4⁺NKG2D⁺ T cells in spleens and tumor tissues. *, $P < 0.05$; **, $P < 0.01$; ***, $P < 0.001$; *ns*, no significance.

anges in CD28 expression were found in the CD4+ T cells of TG, KO, and WT mice (**Figure 4G**). Given that NKG2D is almost not physiologically expressed in CD4+ T cells, miR-16 overexpression in CD4+ T cells does not affect the NKG2D protein level.

B16BL6 or MC38 cells were transplanted into TG mice to evaluate the tumor sensitivity of miR-15a/16TG mice. Compared with those in WT mice, B16BL6 cells grew slightly faster in TG mice particularly at the early phase (from day 8 to 10) (**Figure 4H**). Also, the tumors formed by MC38 cells in TG mice were slightly bigger than those in WT mice (**Figure 4I**). However, no remarkable changes of CD4+ NKG2D+ T cell frequencies were found in the spleens and tumors of both mice (**Figures 4H** and **4I**, S2), indicating that CD4+NKG2D+ T cells are not involved in the tumor-promoting effects in TG mice.

Inefficient induction of CD4+NKG2D+ T cells with miR-15a/16 overexpression

Whether miR-15a/16 overexpression affects the induction of CD4+NKG2D+ T cells through α-CD3/sRAE-1 simulation was analyzed. **Figure 5A** shows that although the CD4+ T cells of wild-type mice showed substantially increased NKG2D expression after the treatments of α-CD3 or α-CD3/sRAE-1, the CD4+ T cells of miR-15a/16TG mice were hardly induced to express NKG2D. TGF-β1 expression was also low in miR-15a/16TG-CD4+ T cells after treatment by α-CD3 or α-CD3/sRAE-1 (**Figure 5B**). However, various treatments did not induce any changes in the CD69, CD44, CD25, CD28, and IL-10 expression of CD4+ T cells between TG and WT mice (**Figures 5C**, S3). This finding indicated the target role of miR-16 on NKG2D expression.

Low miR-16 level of CD4+NKG2D+ T cells involved in CRC progression

Our group previously identified that regulatory CD4+NKG2D+ T cells promote colon cancer growth in mice [27]. Variations of human peripheral blood CD4+NKG2D+ T cells and their miR-16 expression in patients with CRC were then examined. Compared with healthy individuals, patients with CRC had increased frequencies of CD4+NKG2D+ T cells (**Figure 6A**, **6B**) and increased NKG2D expression in their CD4+ T cells. The patients with CRC were then classified into three groups based on Duke's A-D stages. The CD4+NKG2D+ T cell frequencies in the patients from each stage were higher than those in healthy controls (**Figure 6C**), revealing that CD4+NKG2D+ T cells are involved in CRC progression.

The miR-16 level of CD4+NKG2D+ T cells was negatively correlated with the mean fluorescence intensity (MFI) of NKG2D (**Figure 6D**). The miR-16 level was also compared between the CD4+NKG2D+ T and CD4+NKG2D- T cells of the same individual. CD4+NKG2D- T cells displayed higher miR-16 expression than CD4+NKG2D+ T cells (**Figure 6E**). Increased IL-10 and TGF-β1 expression levels were also confirmed in the CD4+NKG2D+ T cells of patients with CRC, particularly those at Duke's C and D stages (**Figure 6F** and **6G**). Besides, the miR-16 level was negatively correlated with IL-10 or TGF-β1 MFI in CD4+NKG2D+ T cells, confirming the role of miR-16 in the immuneregulatory function of CD4+NKG2D+ T cells in CRC.

Discussion

MiR-16 downregulated NKG2D expression via direct binding with its 3'-UTR. MiR-15a/16-deficient mice had many regulatory CD4+ NKG2D+ T cells with tumor-promoting activities. Given that NKG2D is not expressed by physiologic CD4+ T cells, miR-15a/16TG-mice did not display changes in CD4+NKG2D+ T cells. Although fast tumor growth in miR-15a/16TG-mice, the tumor-promoting effects were not involved with CD4+NKG2D+ T cells. NKG2D expression cannot be induced by miR-15a/16 overexpression in CD4+ T cells from the treatment of α-CD3 or α-CD3/sRAE-1 *ex vivo*. These regulatory CD4+NKG2D+ T cells with low miR-16 levels were positively correlated with Duke's CRC stages. The immuneregulatory role of miR-15a/16 in CD4+NKG2D+ T subpopulation was involved in tumor progression.

MiR-15a/16 modulates the balance of regulatory T cells and effector T cells of umbilical cord blood, and its deletion upregulates the umbilical cord blood-derived regulatory T cells via targeting Foxp3 [32]. MiR-16 deficiency also increases the STAT3 expression level and induces regulatory B cells [23]. Here, NKG2D was discovered as a new target of miR-16. Considering the modulation of STAT3 and NF-κB on TGF-β1 transcription [31], the high TGF-

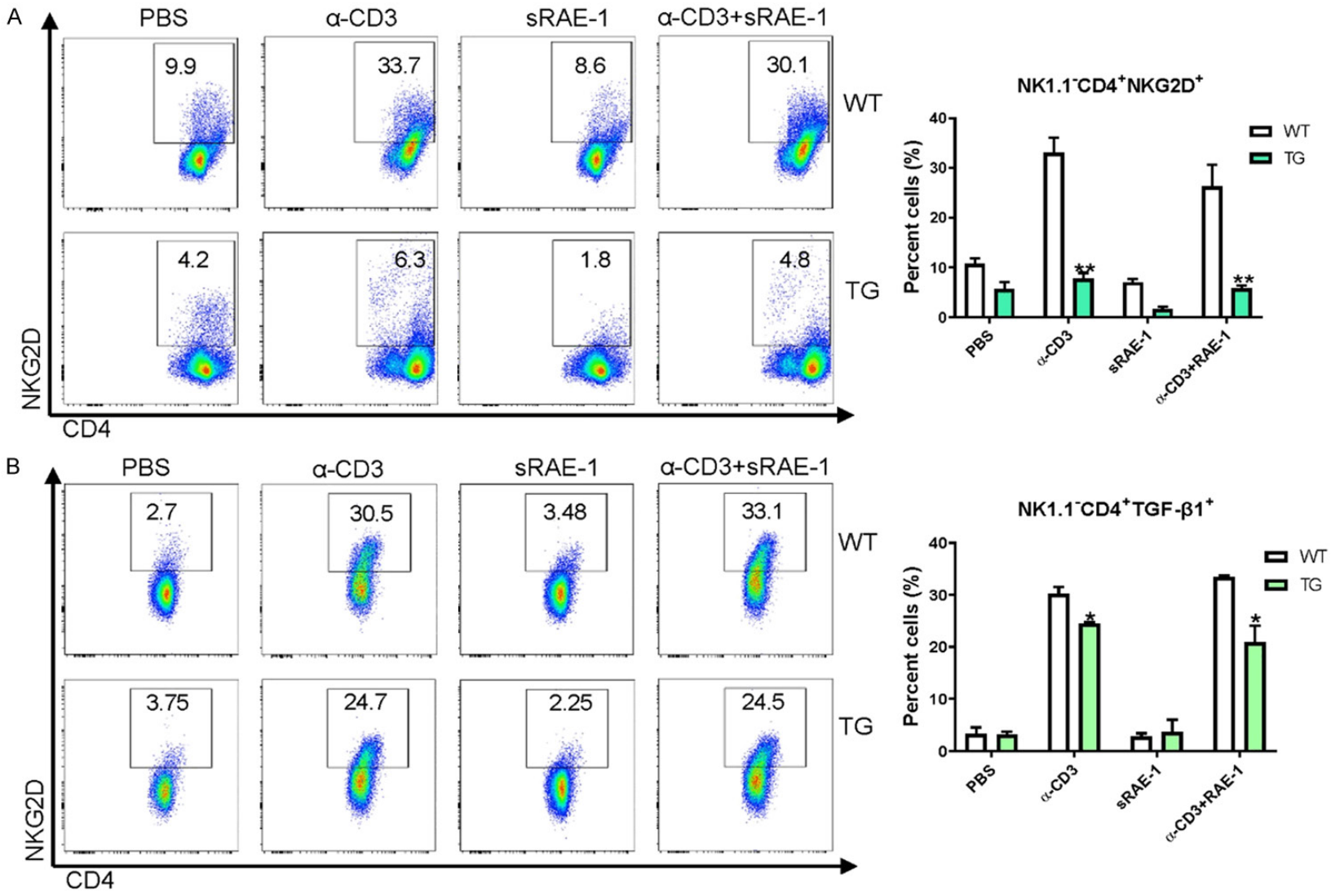
A
PBS
α-CD3
sRAE-1
α-CD3+sRAE-1
9.9
33.7
8.6
30.1
WT
4.2
6.3
1.8
4.8
TG
NKG2D
CD4
NK1.1-CD4+NKG2D+
Percent cells (%)
WT
TG
PBS
α-CD3
sRAE-1
α-CD3+RAE-1
B
2.7
30.5
3.48
33.1
3.75
24.7
2.25
24.5
NK1.1-CD4+TGF-β1+

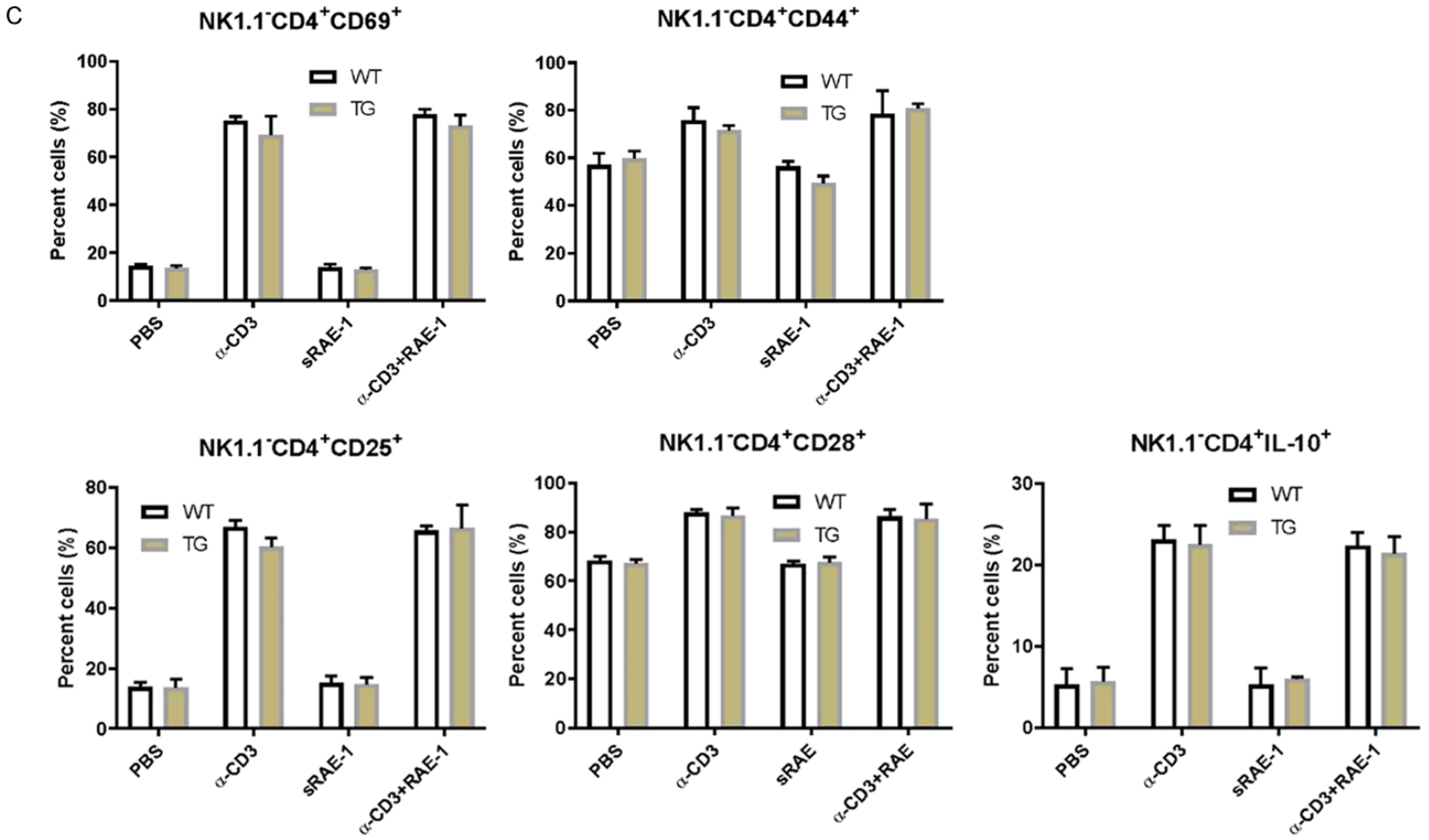

Figure 5. Inefficient induction of miR-15a/16^{TG}-CD4$^+$NKG2D$^+$ T cells *ex vivo*. A. Induced CD4$^+$NKG2D$^+$ T cells of TG mice by α-CD3/sRAE-1. B. TGF-β1 expression on CD4$^+$ T cells treated by α-CD3/sRAE-1. C. Inductions of CD4$^+$CD69$^+$, CD4$^+$CD44$^+$, CD4$^+$CD28$^+$, CD4$^+$CD25$^+$, and CD4$^+$IL-10$^+$ cells. All experiments were conducted at least three times. *, $P < 0.05$; **, $P < 0.01$.

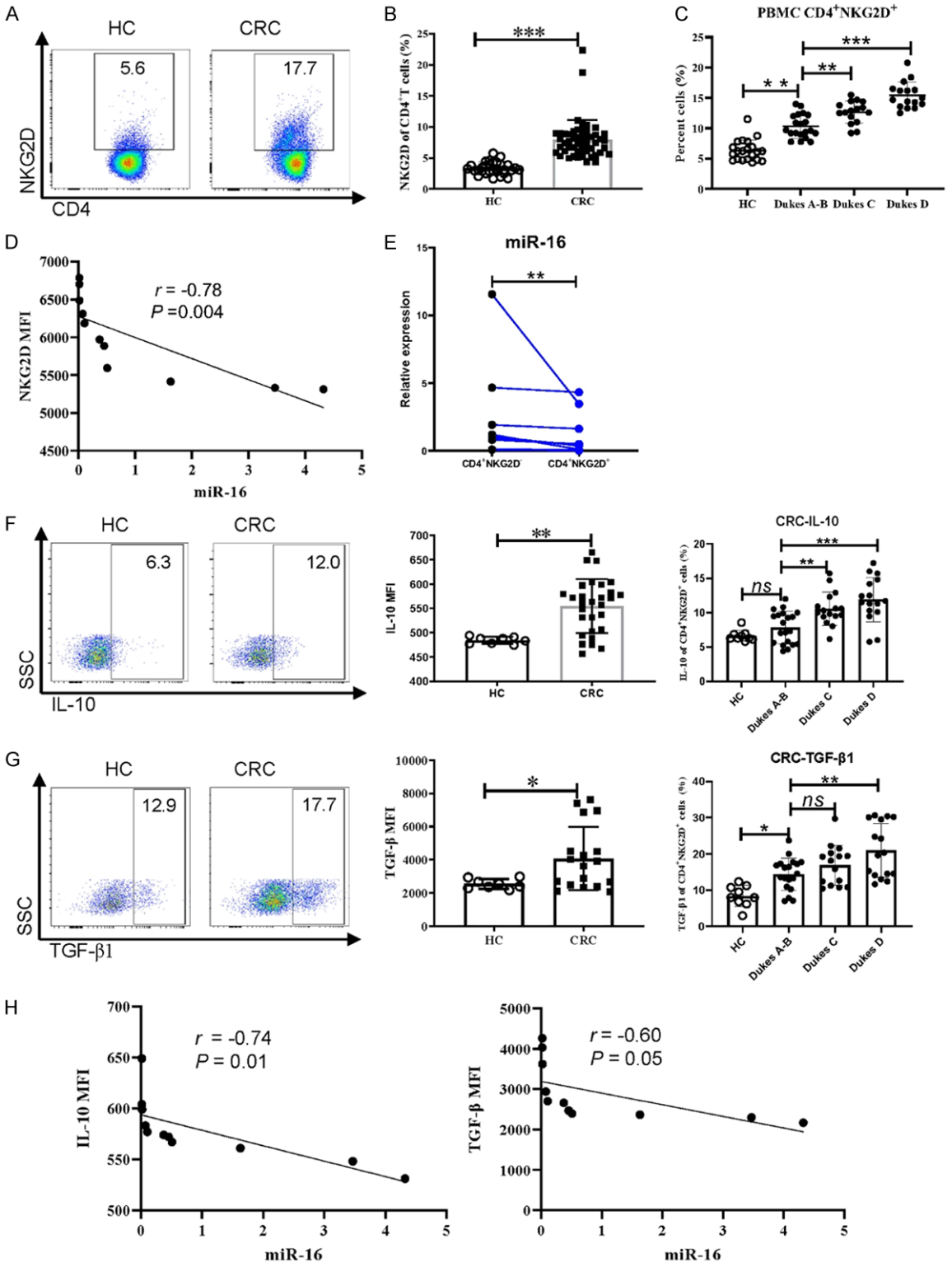

Figure 6. CD4⁺NKG2D⁺ T cells with low miR-16 level involved in CRC progression. (A) NKG2D expression of CD4⁺ T cells in patients with CRC detected by flow cytometry. (B) Elevated NKG2D expression of CD4⁺ T cells indicated by statistical analysis. (C) CD4⁺NKG2D⁺ T cell frequencies in patients with CRC of Duke's A-D stages. (D) Correlation of miR-16 level with NKG2D MFI in CD4⁺NKG2D⁺ T cells. (E) Comparison of miR-16 levels between CD4⁺NKG2D⁺ and CD4⁺NKG2D⁻ T cells in the same individual. IL-10 (F) and TGF-β1 (G) production of CD4⁺NKG2D⁺ T cells in different CRC stages. (H) Correlation of miR-16 level with IL-10 MFI (Left) or TGF-β1 MFI (Right) in CD4⁺NKG2D⁺ T cells of patients with CRC. *, $P < 0.05$; **, $P < 0.01$; ***, $P < 0.001$; *ns*, no significance.

β1 expression of miR-15a/16$^{-/-}$ CD4$^+$NKG2D$^+$ T cells could not cancel the roles of STAT3 and NF-κB. The low miR-16 expression in tumor tissues exhibits dual effects, one is to promote cancer growth and metastasis [2, 3], and the other is to mediate tumor evasion via promoting regulatory CD4$^+$NKG2D$^+$ T, conventional regulatory T (Foxp3$^+$) [32], and regulatory B cells [23].

Given the abundance of regulatory CD4$^+$NKG2D$^+$ T cells at late-stage CRC, efficiently depleting this T cell subpopulation will improve the prognosis of patients with CRC. Although miR-15a/16 deletion induced the CD4$^+$NKG2D$^+$ T cells, miR-16 overexpression did not physiologically affect the activities of these T cell subsets. When tumor cells are transfected with miR-16, tumor cell proliferation is suppressed, but the CD4$^+$NKG2D$^+$ T cells of patients with tumor may not be modulated. Whether the ectopic miR-16 expression decreases the number of regulatory CD4$^+$NKG2D$^+$ T cells, regulatory CD4$^+$Foxp3$^+$ T cells, and regulatory B cells in patients with CRC needs further study. In addition, the miR-16 expression is regulated by multiple factors, such as p53, c-Myc, HIF1, and ATRA [2, 3]. Whether the decreased miR-16 expression of CD4$^+$NKG2D$^+$ T cells in patients with CRC is a result of hypoxic microenvironment or an intrinsic feature of CD4$^+$NKG2D$^+$ T cells requires further clarification.

In summary, miR-16 modulates the activities of regulatory CD4$^+$NKG2D$^+$ T cells, which are positively associated with CRC development. Given the low miR-16 level in multiple tumor cells and regulatory immune cells, gene therapy based on miR-16 transfection will benefit patients with tumor via inhibiting tumor growth and reversing the immune-suppressive microenvironment.

Acknowledgements

This work was supported by the National Natural Science Foundation of China (Grant No. 81671547, 81873866, and 81873867); the "Six peaks" Talent Project of Jiangsu Province; The Natural Science Foundation of Jiangsu Province (BK20180925); Postgraduate Research & Practice Innovation Program of Jiangsu Province, China (Grant No. KYCX_2383).

Disclosure of conflict of interest

None.

Address correspondence to: Drs. Weijuan Gong and Xiaoqin Jia, Jiangsu Key Laboratory of Integrated Traditional Chinese and Western Medicine for Prevention and Treatment of Senile Diseases, Jiangyang Road, Yangzhou, Jiangsu Province, P. R. China. Tel: +86-514-87978820; Fax: +86-514-87341733; E-mail: wjgong@yzu.edu.cn (WJG); xqjia@yzu.edu.cn (XQJ)

References

[1] Calin GA, Dumitru CD, Shimizu M, Bichi R, Zupo S, Noch E, Aldler H, Rattan S, Keating M, Rai K, Rassenti L, Kipps T, Negrini M, Bullrich F and Croce CM. Frequent deletions and down-regulation of micro-RNA genes miR15 and miR16 at 13q14 in chronic lymphocytic leukemia. Proc Natl Acad Sci U S A 2002; 99: 15524-15529.

[2] Pekarsky Y, Balatti V and Croce CM. BCL2 and miR-15/16: from gene discovery to treatment. Cell Death Differ 2018; 25: 21-26.

[3] Huang E, Liu R and Chu Y. miRNA-15a/16: as tumor suppressors and more. Future Oncol 2015; 11: 2351-2363.

[4] Qian J, Jiang B, Li M, Chen J and Fang M. Prognostic significance of microRNA-16 expression in human colorectal cancer. World J Surg 2013; 37: 2944-2949.

[5] Wu WL, Wang WY, Yao WQ and Li GD. Suppressive effects of microRNA-16 on the proliferation, invasion and metastasis of hepatocellular carcinoma cells. Int J Mol Med 2015; 36: 1713-1719.

[6] Jiang QQ, Liu B and Yuan T. MicroRNA-16 inhibits bladder cancer proliferation by targeting cyclin D1. Asian Pac J Cancer Prev 2013; 14: 4127-4130.

[7] Wang F, Mao A, Tang J, Zhang Q, Yan J, Wang Y, Di C, Gan L, Sun C and Zhang H. microRNA-16-5p enhances radiosensitivity through modulating cyclin D1/E1-pRb-E2F1 pathway in prostate cancer cells. J Cell Physiol 2019; 234: 13182-13190.

[8] Kitadate A, Ikeda S, Teshima K, Ito M, Toyota I, Hasunuma N, Takahashi N, Miyagaki T, Sugaya M and Tagawa H. MicroRNA-16 mediates the regulation of a senescence-apoptosis switch in cutaneous T-cell and other non-hodgkin lymphomas. Oncogene 2016; 35: 3692-3704.

[9] Raveche ES, Salerno E, Scaglione BJ, Manohar V, Abbasi F, Lin YC, Fredrickson T, Landgraf P, Ramachandra S, Huppi K, Toro JR, Zenger VE, Metcalf RA and Marti GE. Abnormal microR-

NA-16 locus with synteny to human 13q14 linked to CLL in NZB mice. Blood 2007; 109: 5079-5086.
[10] Shi L, Jackstadt R, Siemens H, Li H, Kirchner T and Hermeking H. p53-induced miR-15a/16-1 and AP4 form a double-negative feedback loop to regulate epithelial-mesenchymal transition and metastasis in colorectal cancer. Cancer Res 2014; 74: 532-542.
[11] Gao SM, Yang J, Chen C, Zhang S, Xing CY, Li H, Wu J and Jiang L. miR-15a/16-1 enhances retinoic acid-mediated differentiation of leukemic cells and is up-regulated by retinoic acid. Leuk Lymphoma 2011; 52: 2365-2371.
[12] Zhang X, Chen X, Lin J, Lwin T, Wright G, Moscinski LC, Dalton WS, Seto E, Wright K, Sotomayor E and Tao J. Myc represses miR-15a/miR-16-1 expression through recruitment of HDAC3 in mantle cell and other non-Hodgkin B-cell lymphomas. Oncogene 2012; 31: 3002-3008.
[13] Dejean E, Renalier MH, Foisseau M, Agirre X, Joseph N, de Paiva GR, Al Saati T, Soulier J, Desjobert C, Lamant L, Prosper F, Felsher DW, Cavaille J, Prats H, Delsol G, Giuriato S and Meggetto F. Hypoxia-microRNA-16 downregulation induces VEGF expression in anaplastic lymphoma kinase (ALK)-positive anaplastic large-cell lymphomas. Leukemia 2011; 25: 1882-1890.
[14] Cui X, Witalison EE, Chumanevich AP, Chumanevich AA, Poudyal D, Subramanian V, Schetter AJ, Harris CC, Thompson PR and Hofseth LJ. The induction of microRNA-16 in colon cancer cells by protein arginine deiminase inhibition causes a p53-dependent cell cycle arrest. PLoS One 2013; 8: e53791.
[15] Cittelly DM, Das PM, Salvo VA, Fonseca JP, Burow ME and Jones FE. Oncogenic HER2{delta} 16 suppresses miR-15a/16 and deregulates BCL-2 to promote endocrine resistance of breast tumors. Carcinogenesis 2010; 31: 2049-2057.
[16] Chen CQ, Chen CS, Chen JJ, Zhou LP, Xu HL, Jin WW, Wu JB and Gao SM. Histone deacetylases inhibitor trichostatin A increases the expression of Dleu2/miR-15a/16-1 via HDAC3 in non-small cell lung cancer. Mol Cell Biochem 2013; 383: 137-148.
[17] Sampath D, Liu C, Vasan K, Sulda M, Puduvalli VK, Wierda WG and Keating MJ. Histone deacetylases mediate the silencing of miR-15a, miR-16, and miR-29b in chronic lymphocytic leukemia. Blood 2012; 119: 1162-1172.
[18] Liang X, Xu Z, Yuan M, Zhang Y, Zhao B, Wang J, Zhang A and Li G. MicroRNA-16 suppresses the activation of inflammatory macrophages in atherosclerosis by targeting PDCD4. Int J Mol Med 2016; 37: 967-975.
[19] Chen T, Xiao Q, Wang X, Wang Z, Hu J, Zhang Z, Gong Z and Chen S. miR-16 regulates proliferation and invasion of lung cancer cells via the ERK/MAPK signaling pathway by targeted inhibition of MAPK kinase 1 (MEK1). J Int Med Res 2019; 47: 5194-5204.
[20] Zhang K, Han Y, Zhao Y, Sun Y, Zou M, Fu Y and Peng X. Upregulated gga-miR-16-5p inhibits the proliferation cycle and promotes the apoptosis of MG-infected DF-1 cells by repressing PIK3R1-mediated the PI3K/Akt/NF-kappaB pathway to exert anti-inflammatory effect. Int J Mol Sci 2019; 20: 1036.
[21] Jia X, Hu X, Han S, Miao X, Liu H, Li X, Lin Z, Wang Z and Gong W. Increased M1 macrophages in young miR-15a/16(-/-) mice with tumour grafts or dextran sulphate sodium-induced colitis. Scand J Immunol 2018; 88: e12703.
[22] Kasar S, Underbayev C, Yuan Y, Hanlon M, Aly S, Khan H, Chang V, Batish M, Gavrilova T, Badiane F, Degheidy H, Marti G and Raveche E. Therapeutic implications of activation of the host gene (Dleu2) promoter for miR-15a/16-1 in chronic lymphocytic leukemia. Oncogene 2014; 33: 3307-3315.
[23] Jia X, Liu H, Xu C, Han S, Shen Y, Miao X, Hu X, Lin Z, Qian L, Wang Z and Gong W. MiR-15a/16-1 deficiency induces IL-10-producing CD19(+) TIM-1(+) cells in tumor microenvironment. J Cell Mol Med 2019; 23: 1343-1353.
[24] Marcais A, Blevins R, Graumann J, Feytout A, Dharmalingam G, Carroll T, Amado IF, Bruno L, Lee K, Walzer T, Mann M, Freitas AA, Boothby M, Fisher AG and Merkenschlager M. microRNA-mediated regulation of mTOR complex components facilitates discrimination between activation and anergy in CD4 T cells. J Exp Med 2014; 211: 2281-2295.
[25] Li T, Morgan MJ, Choksi S, Zhang Y, Kim YS and Liu ZG. MicroRNAs modulate the noncanonical transcription factor NF-kappaB pathway by regulating expression of the kinase IKKalpha during macrophage differentiation. Nat Immunol 2010; 11: 799-805.
[26] Gagnon JD, Kageyama R, Shehata HM, Fassett MS, Mar DJ, Wigton EJ, Johansson K, Litterman AJ, Odorizzi P, Simeonov D, Laidlaw BJ, Panduro M, Patel S, Jeker LT, Feeney ME, McManus MT, Marson A, Matloubian M, Sanjabi S and Ansel KM. miR-15/16 restrain memory T cell differentiation, cell cycle, and survival. Cell Rep 2019; 28: 2169-2181, e2164.
[27] Lin Z, Han S, Qian X, Hu C, Xiao W, Qian L, Zhang Y, Ding Y, Jia X, Zhu G and Gong W. Regulatory NK1.1(-) CD4(+) NKG2D(+) subset induced by NKG2DL(+) cells promotes tumor evasion in mice. Cancer Immunol Immunother 2018; 67: 1159-1173.

[28] Qian X, Hu C, Han S, Lin Z, Xiao W, Ding Y, Zhang Y, Qian L, Jia X, Zhu G and Gong W. NK1.1(-) CD4(+) NKG2D(+) T cells suppress DSS-induced colitis in mice through production of TGF-beta. J Cell Mol Med 2017; 21: 1431-1444.

[29] Lin Z, Wang C, Xia H, Liu W, Xiao W, Qian L, Jia X, Ding Y, Ji M and Gong W. CD4(+) NKG2D(+) T cells induce NKG2D down-regulation in natural killer cells in CD86-RAE-1epsilon transgenic mice. Immunology 2014; 141: 401-415.

[30] Han S, Zhu T, Ding S, Wen J, Lin Z, Lu G, Zhang Y, Xiao W, Ding Y, Jia X, Chen H and Gong W. Early growth response genes 2 and 3 induced by AP-1 and NF-kappaB modulate TGF-beta1 transcription in NK1.1(-) CD4(+) NKG2D(+) T cells. Cell Signal 2020; 76: 109800.

[31] Han S, Ding S, Miao X, Lin Z, Lu G, Xiao W, Ding Y, Qian L, Zhang Y, Jia X, Zhu G and Gong W. TGF-beta1 expression in regulatory NK1.1(-) CD4(+) NKG2D(+) T cells dependents on the PI3K-p85alpha/JNK, NF-kappaB and STAT3 pathways. Am J Cancer Res 2018; 8: 489-501.

[32] Liu X, Robinson SN, Setoyama T, Tung SS, D'Abundo L, Shah MY, Yang H, Yvon E, Shah N, Yang H, Konopleva M, Garcia-Manero G, McNiece I, Rezvani K, Calin GA, Shpall EJ and Parmar S. FOXP3 is a direct target of miR15a/16 in umbilical cord blood regulatory T cells. Bone Marrow Transplant 2014; 49: 793-799.

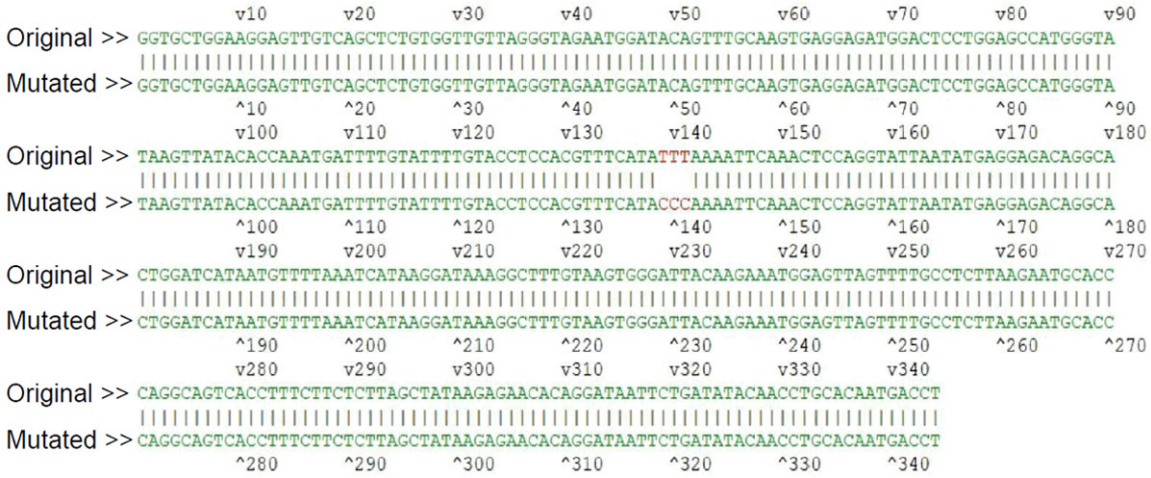

Figure S1. Mutated nucleotides in 3'-UTR of the NKG2D gene.

Table S1. Clinical characteristics of colorectal cancer patients

Characteristics	Number	Dukes			χ^2	P
		A-B	C	D		
Age						
< 60	9	3	4	2	0.9943	0.6083
≥ 60	43	17	12	14		
Gender						
Male	35	14	11	10	0.2491	0.8829
Female	17	6	5	6		
Site						
Left	25	11	6	8	1.125	0.5699
Right	27	9	10	8		
Invasion depth						
< serosa	8	7	0	1	9.846	0.0073
≥ serosa	44	13	16	15		
Lymph node metastasis						
No	24	20	1	3	28.53	< 0.0001
Yes	28	0	15	13		
Distant metastasis						
No	35	20	15	0	47.742	< 0.0001
Yes	17	0	1	16		
Differentiation						
Well	13	1	6	6	7.7914	0.0995
Moderate	37	18	9	10		
Poor	2	1	1	0		
CEA	46.32±157.81	7.04±7.77	7.28±10.08	134.46±269.31	P_{AB-C} = 0.2828 P_{AB-D} = 0.0411 P_{C-D} = 0.0688	
CA199	67.95±133.35	33±70.02	32.97±26.69	146.61±209.76	P_{AB-C} = 0.9985 P_{AB-D} = 0.0293 P_{C-D} = 0.0397	

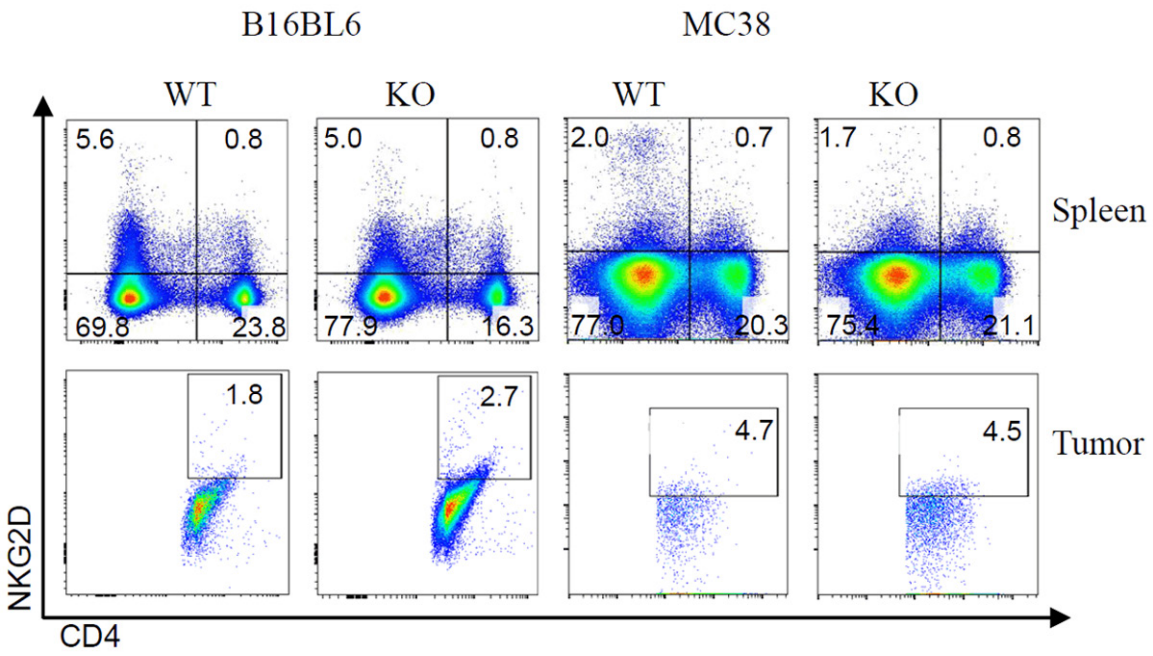

Figure S2. Representative results of NK1.1⁻CD4⁺NKG2D⁺ cells in spleens and tumor stransplanted with B16BL6 or MC38 cells.

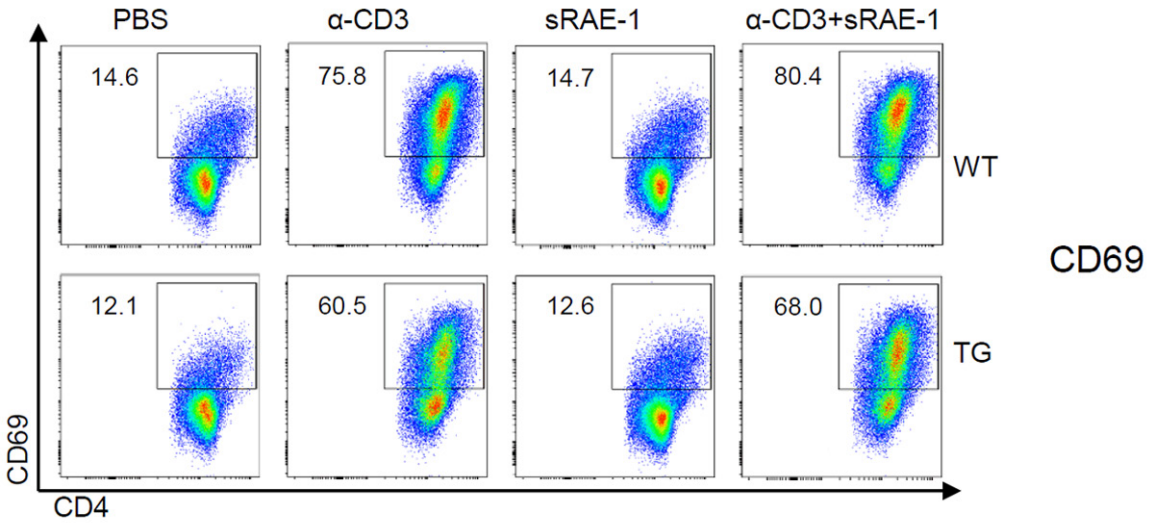

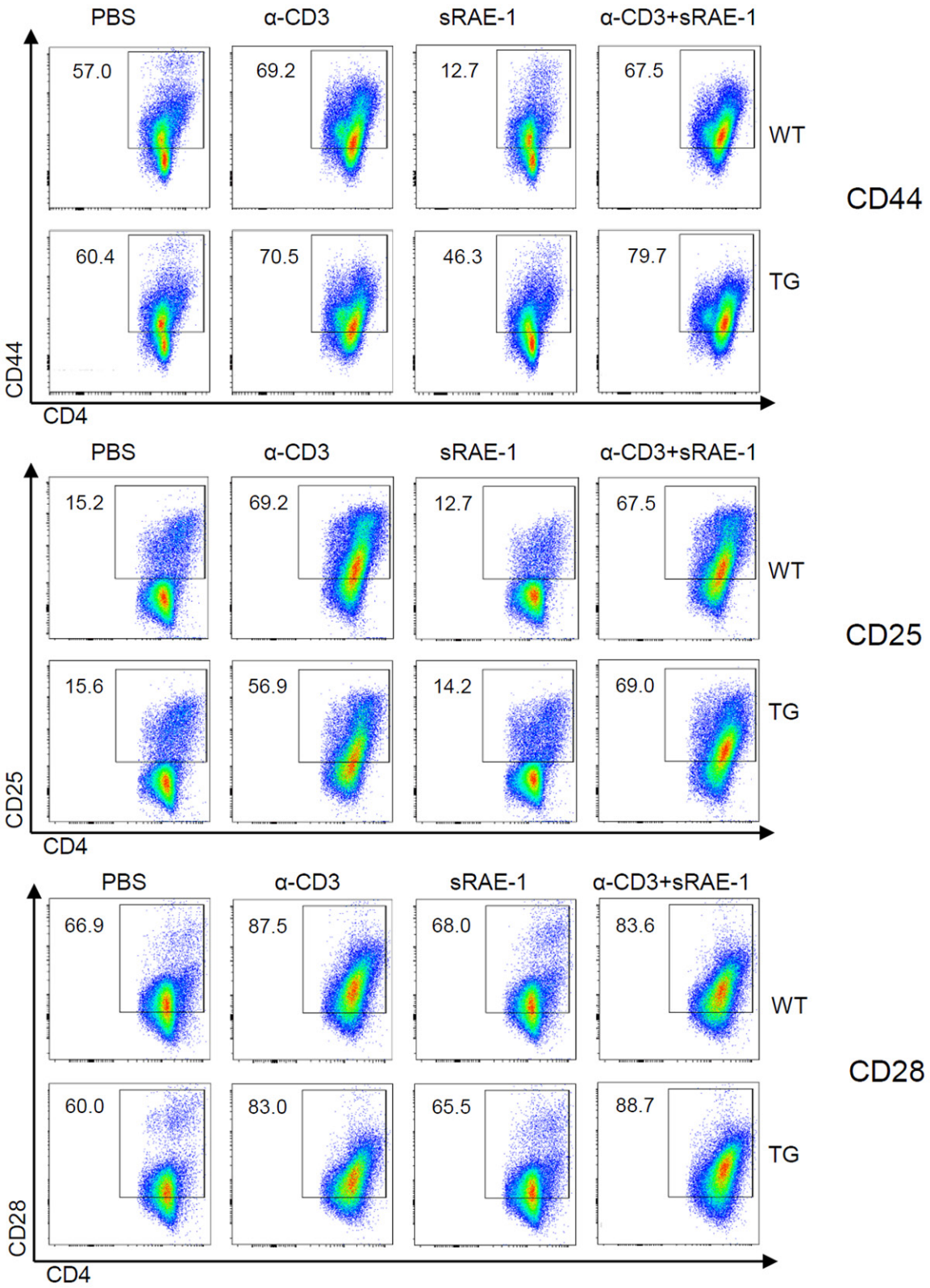

Figure S3. Representative results of *in vitro* activation of WT/TG-CD4⁺ T cells with α-CD3, sRAE-1, or α-CD3 plus sRAE-1.